

UA Demonstration Module Description

RS661
UNIVERSITY ALLIANCE

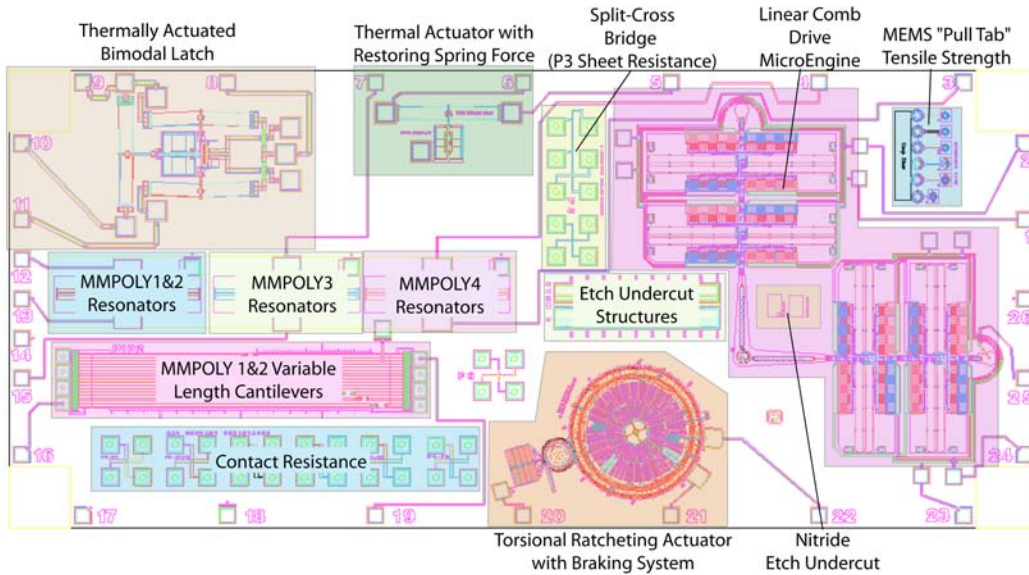


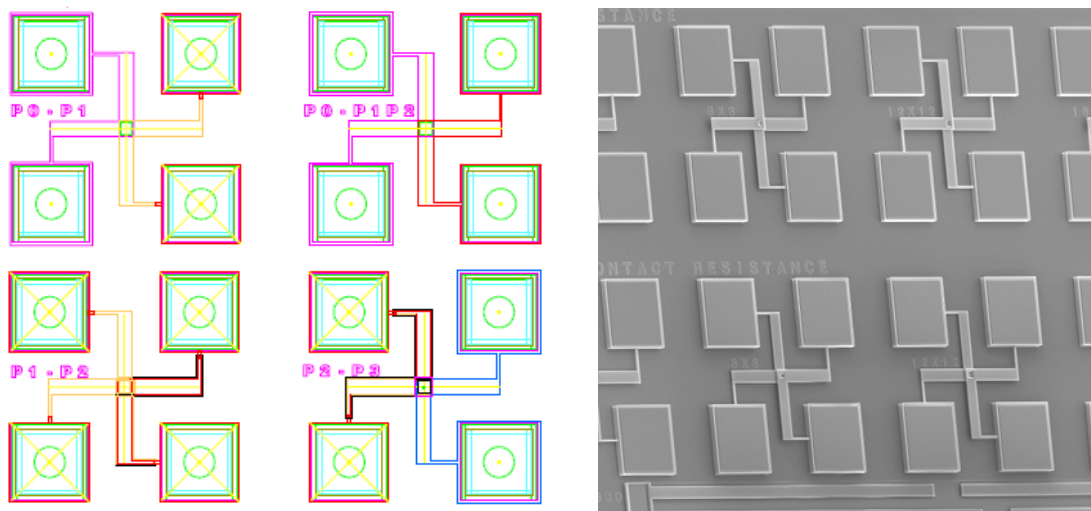
TABLE OF CONTENTS

TABLE OF CONTENTS	2
CONTACT RESISTANCE	4
OPERATION	4
TECHNICAL DETAILS	5
<i>Greek Cross</i>	5
<i>Reference</i>	6
ETCH UNDERCUT AND NITRIDE ETCH UNDERCUT STRUCTURES	6
<i>Reference</i>	7
LINEAR COMB DRIVE MICRO ENGINE	7
OPERATION	8
<i>Notes:</i>	9
TECHNICAL DETAILS	9
<i>Reference</i>	11
MEMS “PULL TAB” TENSILE STRENGTH STRUCTURES	12
OPERATION	12
TECHNICAL DETAILS	13
<i>Reference</i>	13
RESONATOR	14
OPERATION	15
<i>Procedure</i>	15
TECHNICAL DETAILS	17
<i>NOMENCLATURE</i>	17
<i>Reference</i>	19
SPLIT-CROSS BRIDGE	20
OPERATION	20
TECHNICAL DETAILS	21
<i>Calculating Sheet Resistance</i>	21
<i>Calculating Linewidth</i>	21
<i>Measuring the Overlay Error</i>	21
<i>Reference</i>	22
THERMAL ACTUATOR WITH RESTORING SPRING FORCE	23
OPERATION	23
TECHNICAL DETAILS	24
<i>Young’s Modulus</i>	24
<i>Resistivity</i>	24
<i>Thermal Conductivity</i>	24
<i>Coefficient of Thermal Expansion (CTE)</i>	24
<i>Using Euler Column Formula for Buckling:</i>	25
<i>Reference</i>	27
THERMALLY ACTUATED LATCHING SWITCH	28
OPERATION	30
TECHNICAL DETAILS	31
TORSIONAL RATCHET ACTUATOR WITH BRAKING SYSTEM (TRA)	32

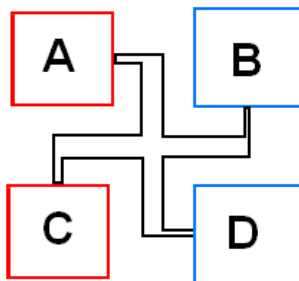
OPERATION	33
TECHNICAL DETAILS	33
<i>Reference</i>	34
VARIABLE LENGTH CANTILEVERS	35
OPERATION	35
TECHNICAL DETAILS	36
<i>To Find Surface Adhesion</i>	<i>Error! Bookmark not defined.</i>
<i>To Measure Z-axis Stress Gradient</i>	36
<i>Reference</i>	36
UA MODULE BOND PAD LEGEND.....	37
REFERENCES:.....	38

Contact Resistance

The cross shaped structures shown below were designed to measure the resistance of the fabricated connection, or "contact," between two poly layers. A poly-on-poly "contact" of this type is not the same as a probe contact on a probe pad or ohm-meter leads contacting a resistor. This is because, in the absence of any fabrication errors, the two layers in the process are physically grown together. So the test structure is really testing the continuity through this connection. If there were a fabrication error, for example the Sacox_Cut did not clear out completely, then this poly-to-poly connection measurement would be large.



Operation



Measurement	Applied 1 mA Of Current	Measurement Of Voltage
1	C → D	A → B
2	D → C	A → B
3	A → B	C → D
4	B → A	C → D

To find the contact resistance four measurements need to be taken. A current of 1 mA is applied between the C-D pads and the voltage between the A-B pads is taken. Then, the direction of the current is reversed and the voltage is read again. Finally, the current is applied between the A-B pads and the voltage between the C-D pads is taken, again with current in one direction and then the other.

Technical Details

Bad contacts are the cause of failure or poor performance in a wide variety of electrical devices. For example, a sufficiently high contact resistance can cause substantial heating in a high current device. Unpredictable or noisy contacts are a major cause of the failure of electrical equipment. An intermittent contact which alternates rapidly between a high and low resistance can be extremely difficult to troubleshoot.

Greek Cross

This four pad structure is also known as a Greek cross. It is used to determine sheet resistance. Sheet resistance can be measured at the center of the cross to an accuracy of 0.1%.

$$R = \frac{V_{\text{between pads D and C}}}{I_{\text{between pads A and D}}}$$

$$R = \frac{\pi R_s}{\ln 2}$$

Another more accurate way to measure the sheet resistance is by taking an initial measurement and then taking a second reversed measurement. See reciprocity theorem shown below:

$$R_{AB,CD} = R_{CD,AB}$$

$$R_{\text{initial}} = \frac{V_{\text{between D and C}} - V_{\text{between C and D}}}{I_{\text{between A and B}} - I_{\text{between B and A}}}$$

$$R_{\text{rotated } 90^\circ} = \frac{V_{\text{between A and D}} - V_{\text{between D and A}}}{I_{\text{between B and C}} - I_{\text{between C and B}}}$$

The Average Resistance:

$$R = \frac{R_{\text{initial}} + R_{\text{rotated } 90^\circ}}{2}$$

The Sheet Resistance:

$$R_s = \frac{\pi R}{\ln 2}$$

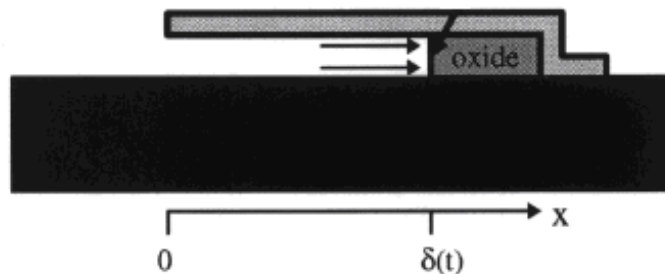
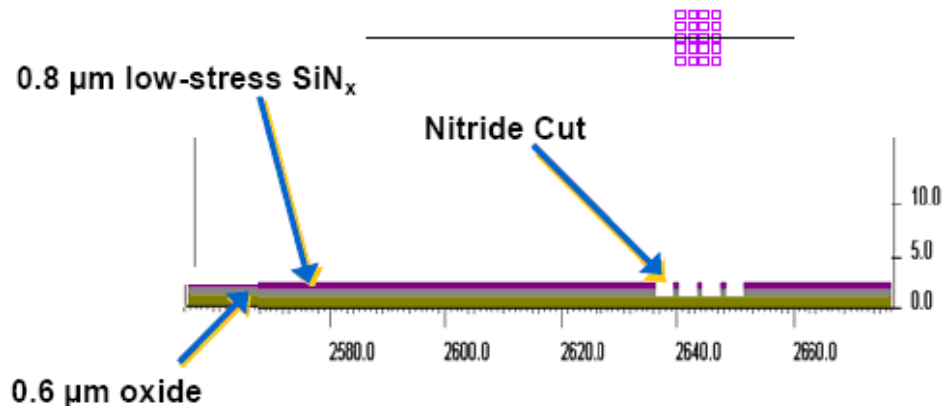
Reference

Schroder, Dieter K. Semiconductor Material and Device Characterization. New York: John Wiley & Sons, Inc., 1990. 1-14.

“Microelectronic Test Structures” *A.J. Walton*, Edinburgh Microfabrication Facility
Department of Electrical Engineering Kings Buildings, University of Edinburgh
Edinburgh, EH9 3JL, UK <www.see.ed.ac.uk/research/IMNS/papers/micro_test.pdf>.

Etch Undercut and Nitride Etch Undercut Structures

Etch undercut structures are usually on each design, as part of a process control. During production the staff can make sure that the release-etch process is within parameters. They do this by examining the etching lines. Essentially a large “tunnel” capped with polysilicon and initially filled with oxide is used. After release, the structures may be examined under a dark-field microscope to see how far the oxide has been etched into the tunnel. As the release-etch time increases the test structure will be undercut further. By observing how far the oxide material has been undercut in a specific amount of time the process can be tailored.

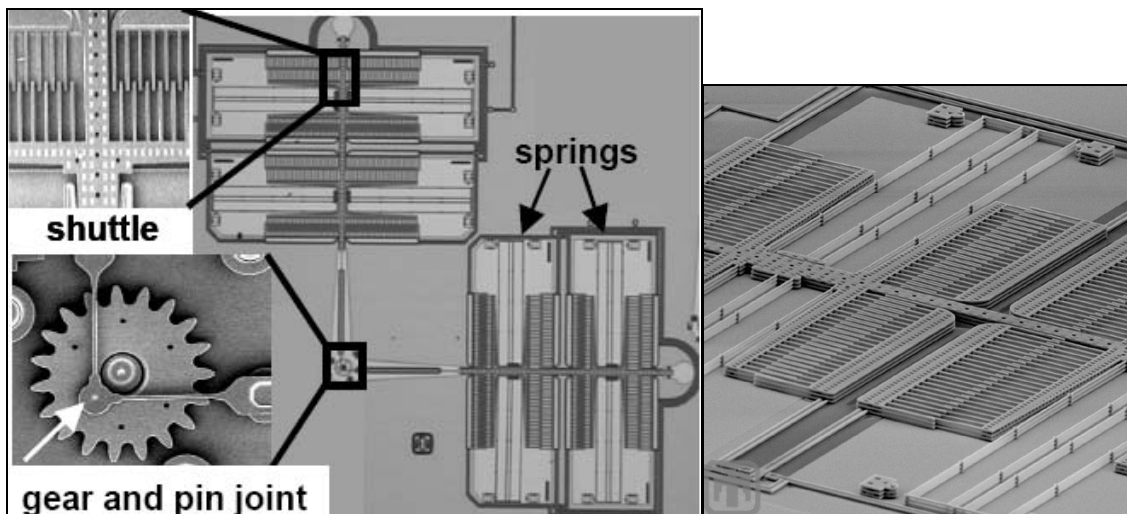


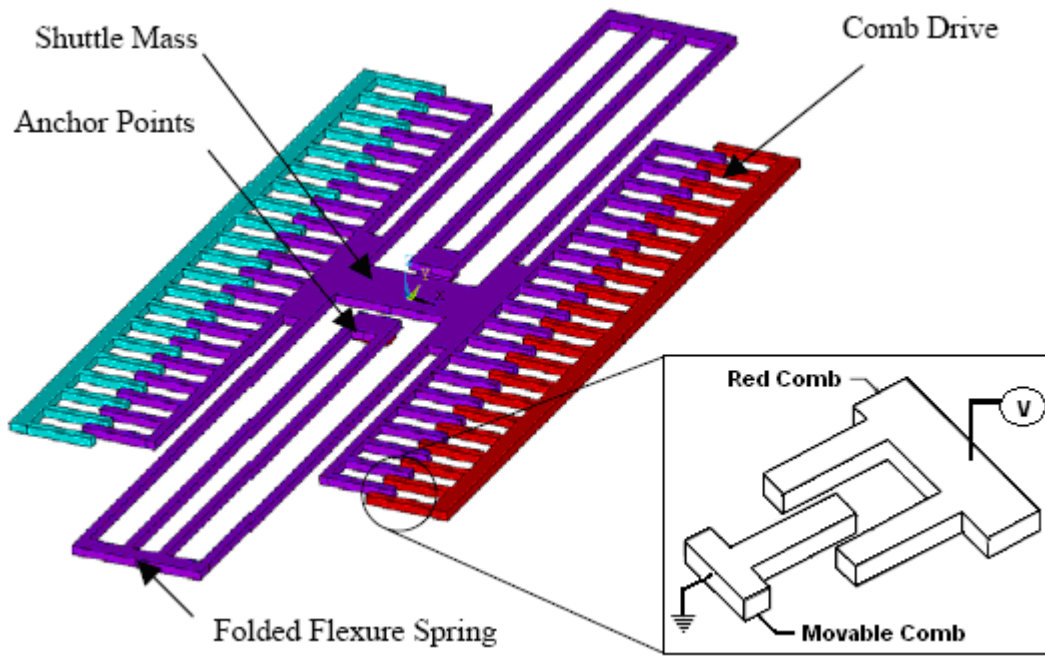
Reference

“Release-etch modeling for complex surface micromachined structures”, W.P. Eaton, J.H. Smith, R.L. Jarecki, Sandia National Laboratories, Micromachined Devices and Components, Proceedings of the SPIE, Vol 2882, Austin, TX, Oct 14-15, 1996

Linear Comb Drive Micro Engine

The microengine is made up of two perpendicular comb-drive actuators. These actuators are attached to a center, rotating gear. The center gear rotates around a hub, which is attached to the substrate by a pin joint.





Operation

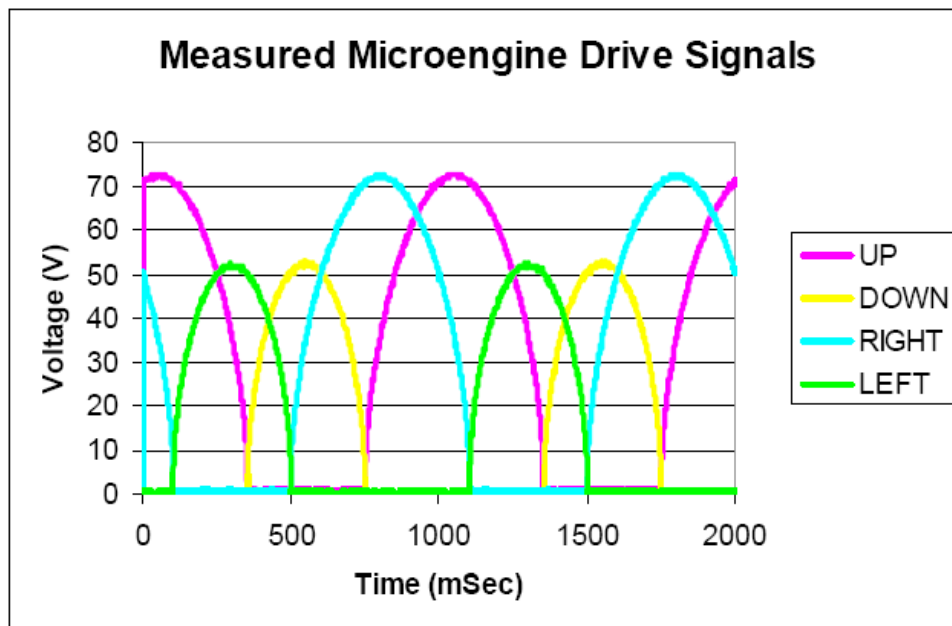
Bond Pad Information					
Bond Pad Number	Input Signal Label	Input Signal Frequency	Input Voltage Peak to Peak	Waveform	Other
*Bond Pad Directly Across from Bond Pad 1	Down	0.1 to 2400Hz	52.5	Clipped Sine	180° out of phase with "up"
*Bond Pad Directly Across from Bond Pad 2	Up	0.1 to 2400Hz	72.5	Clipped Sine	180° out of phase with "down"
23	Left	0.1 to 2400Hz	52.5	Clipped Sine	180° out of phase with "right"
24	Right	0.1 to 2400Hz	72.5	Clipped Sine	180° out of phase with "left"
25	Ground	NA	NA	NA	

*Note- Although Bond Pads 1 and 2 are acceptable for use, to alleviate the spatial constraints posed by using pads 1 and 2; it is suitable to place the needed probe tips on the bond pads directly across from pads 1 and 2.

Operating Signals: four phase-separated drive signals:

“up” and “down” signals are both are clipped sine waves, 180 degrees out of phase
“left” and “right” signals are both are clipped sine waves, 180 degrees out of phase
Resonance frequency for this Microengine design is approximately 10500 Hz.

By applying the proper drive voltages to the four inputs, the linear displacement is transformed into circular motion. The Sandia microengine requires four phase-separated drive signals for normal operation. Electrostatically driven microengines utilize electrostatic attraction that results from an electric field between two objects at different potentials to induce motion. These electrostatic forces attract but do not repel. For this reason, banks on opposite sides of the shuttle are required to displace the shuttle in both directions from its fabricated equilibrium position. The figure below illustrates the drive signals utilized in the Microengine.

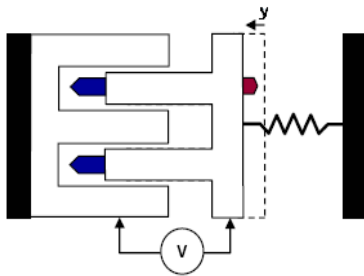
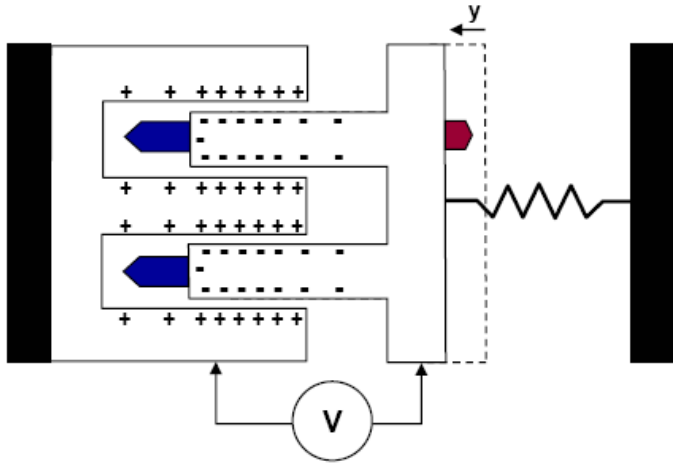


Notes:

1. Be cautious of electrostatic discharge (ESD) when handling all MEMS devices.
2. Be cautious of voltage spikes from powering equipment on and off (always raise your probe tips).

Technical Details

A voltage difference produces an attractive force between the combs:

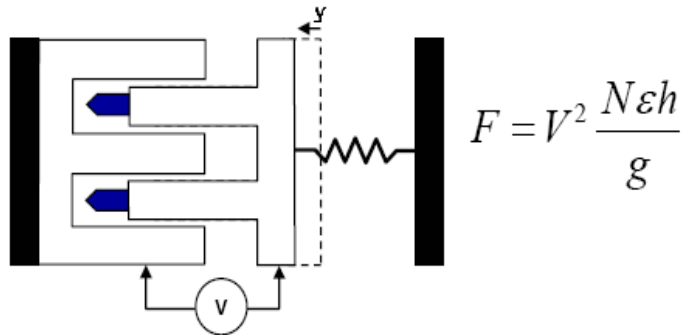


$$F = V^2 \frac{N\epsilon h}{g}$$

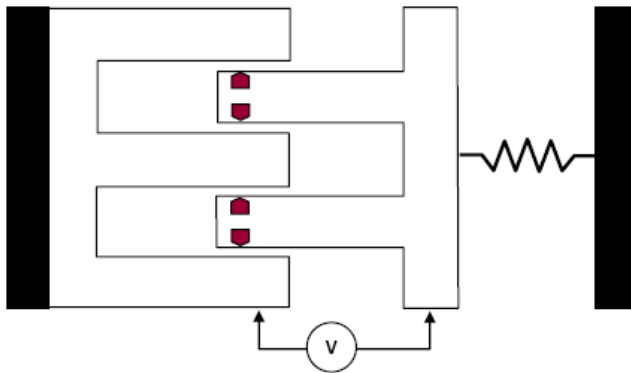
- V Voltage (V)
- N Number of combs
- ϵ Dielectric Constant (F/m)
- h Vertical height of combs (m)
- g Gap between combs (m)

This calculation ignores fringe fields which can be important

There are perpendicular forces between the combs:



- Uniform force – does not depend on how far comb moves
- Increases with square of applied voltage
- Increases as gap between combs decreases
- Typically get micro-Newtons of force



If exactly centered, forces are equal and opposite. However, this is an unstable equilibrium – a slight displacement could lead to clamping

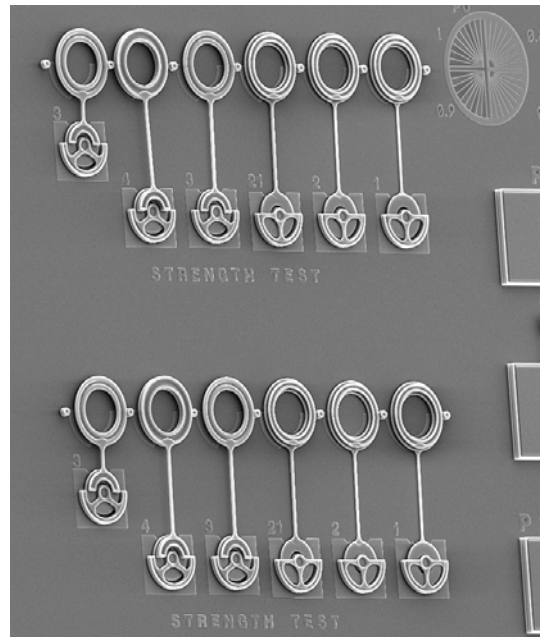
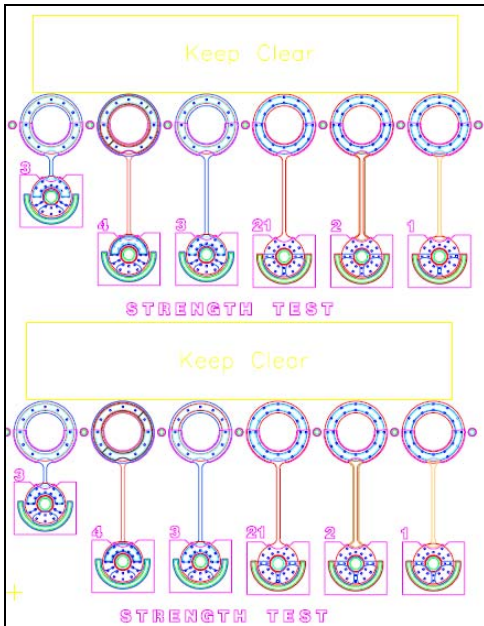
Reference

Image from: Moussa, W.A., H Ahmed, W Badawy, et al. "Investigating the Reliability of Electrostatic Comb-Drive Actuators Used in Microfluidic and Space Systems Using Finite Element Analysis." Canadian Journal of Electrical and Computer Engineering 27 (2002): 195-200.

Ted Dellin "Electrostatics and Comb Drives" Power Point, 2005

MEMS “Pull Tab” Tensile Strength Structures

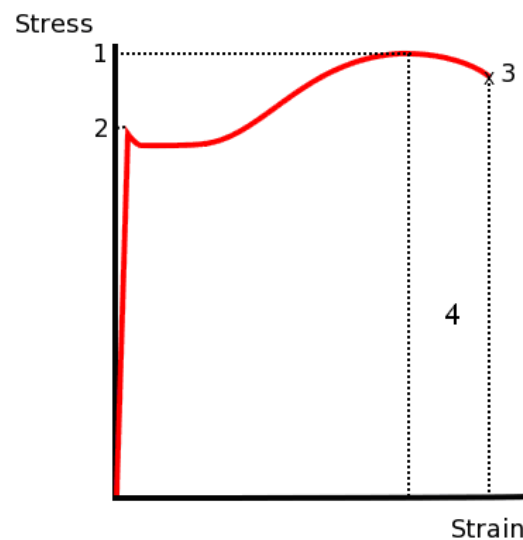
These “Pull Tab” tensile strength structures are used to directly measure modulus and fracture strength which allows elastic properties to be determined. Ultimate tensile strength σ_{UTS} , or S_U measures the force required to pull an object to the point where it breaks.



Operation

A lateral force experiment is performed in a nano-indenter. The pull-tab is engaged with a flat bottomed, conical diamond while the stage is translated. Displacement, normal force and lateral force data is recorded, and then converted to a stress-strain curve using the dimensions of the sample; accurate dimensions are important for analysis.

1. Ultimate Strength
2. Yield Strength
3. Rupture/Breaking Point
4. Necking region



Technical Details

$$\text{Stress} = \frac{\text{Applied Load}}{\text{Cross - Sectional Area}} = \sigma$$

$$\text{Strain} = \frac{\text{Change in Length of Material}}{\text{Original Length of Material}} = \epsilon$$

$$\text{Young's Modulus} = \frac{\text{Stress}}{\text{Strain}} = \frac{\sigma}{\epsilon} = E$$

Ultimate strength is the maximum stress a material can handle when a load is applied to it. This can be found by:

$$\frac{\text{Load at Failure}}{\text{Original Cross - Sectional Area}}$$

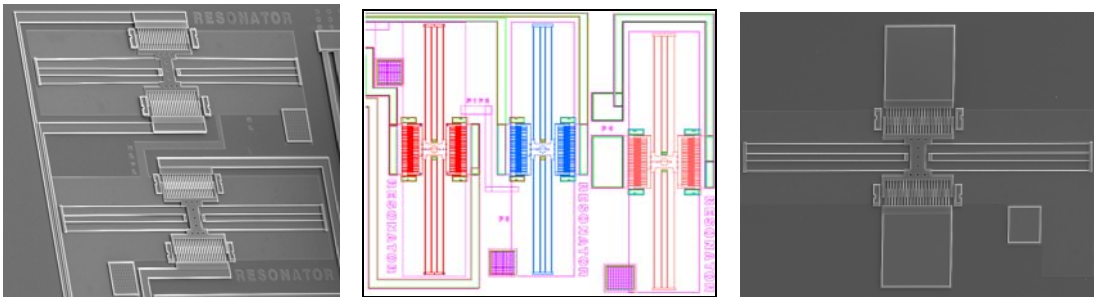
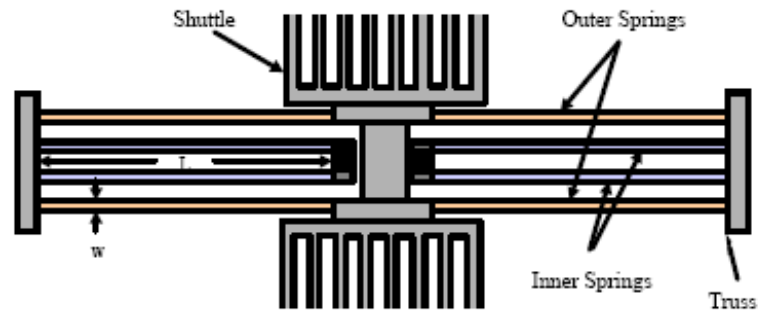
Necking is visible when a ductile material's stress goes past the material's ultimate strength. The material's width will become thinner, while its length becomes longer before it fails completely and ruptures. When a load is applied there is a point at which the material is permanently, plastically, deformed even if the load is removed. When this happens the material had reached its elastic limit, and the value at this point is called yield strength.

Reference

Beer, Ferdinand P., and Russell Johnston Jr. Mechanics of Materials. 2nd ed. New York: McGraw-Hill, Inc., 1992. 24-47.

Resonator

The frequency at which a system oscillates at maximum amplitude is known as the system's resonance frequency. When damping is small, the resonance frequency is approximately equal to the natural frequency of the system, which is the frequency free of vibrations. MEMS surface-micromachining fabrication requires the use of many different tools to deposit thin-films, precisely define patterns using typical photolithography and perform etching processes. As with any fabrication process there is inherent variation, which is acceptable when controlled within suitable limits. By measuring the resonance frequency of the comb drives the overall process uniformity from lot to lot can be seen. Although directly dependent on mass and spring constant, a measure of the resonant frequencies generally provides a good indicator of both process repeatability and geometric variation.



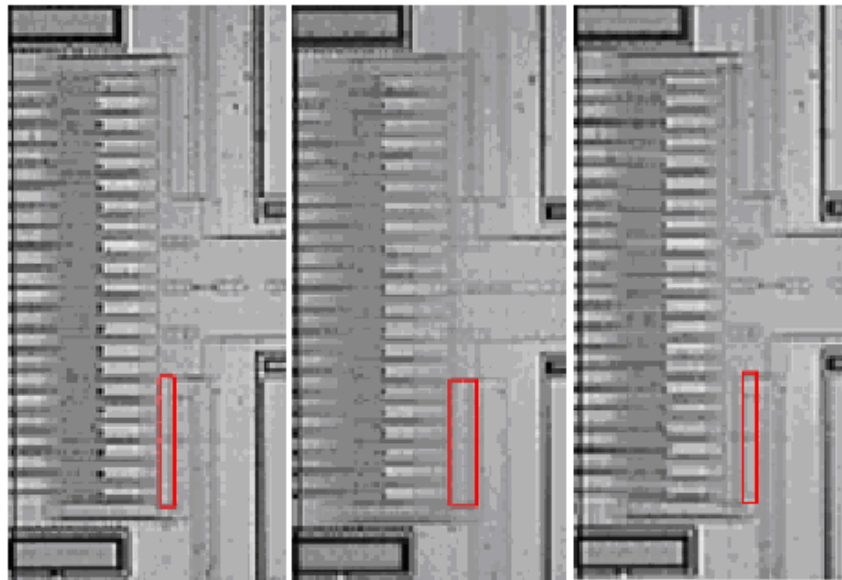
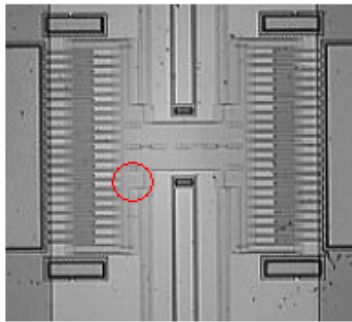
Operation

Device	Bond Pad Number	Input Signal	Input Signal Frequency	Input Voltage Peak to Peak	Waveform	Other
Left	13	Input	Vary, until visual displacement is greatest	~40V	Sine	Offset sine voltage by +20 so that wave minimum = 0 V
Left	12	Ground	NA	NA	NA	
Middle	15	Input	Vary, until visual displacement is greatest	~40V	Sine	Offset sine voltage by +20V so that wave Minimum = 0V
Middle	7	Ground	NA	NA	NA	
Right	3	Input	Vary, until visual displacement is greatest	~40	Sine	Offset sine voltage by +20 so that wave minimum = 0 V
Right	4	Ground	NA	NA	NA	

To study the geometric variation on the wafer, the “blur envelope” method for determining resonant frequency is used. This method produces fast and repeatable measurements. For this method, an adjustable electrical drive signal (sine wave) is used. By holding the drive signal amplitude constant and carefully adjusting its frequency the resonant frequency can be determined. The frequency, at which the comb drive resonator experiences the largest visual displacement, is the resonant frequency.

Procedure for the Blurred Envelope Technique for Determining Resonant Frequency of a Device

1. Apply a sinusoidal voltage of 40 V_{peak to peak} to one of the comb drive pads
2. Offset sinusoidal voltage by +20V so that the minimum in the sine wave is zero volts
3. The other pad and the underlying ground plane are grounded
4. Slowly increase the frequency of the signal, while visually observing the motion of the comb drive
5. The frequency at which the amplitude of motion is the greatest is the resonant frequency



Comb Drive, with area of interest circled in red (top) Enlarged left-half of a comb drive before resonant frequency (left). At resonant frequency with maximum displacement (middle). After resonant frequency, returned to original position (right).

Technical Details

NOMENCLATURE

ω_0	Resonant Frequency (Hz)	L	Spring Length (μm)
E	Youngs Modulus of Elasticity (Pa)	w	Spring Width (μm)
I	Monment of Inertia (μm^4)	t	Layer Thickness (μm)
F	Force (N)	K	Spring Constant
M_{eff}	Effective Resonator Mass (kg)	K_{eff}	Effective Spring Constant
A_{eff}	Effective Resonator Area (μm^2)	ρ	Density (kg/m^3)
V	Voltage (Volts)	R_s	Sheet Resistance (Ohms/Square)
I	Current (Ohms Ω)	n	Number of Comparisons Made
x	Calculated Spring Width (μm)	y	Measured Linewidth (μm)

A mathematical model was derived to predict the undamped resonant frequency of the comb-drive resonators. Resonant frequency (ω_0) is directly dependent on mass and spring constant.

Resonant frequency = (ω_0)

Spring constant = (K_{eff})

Mass constant = (M_{eff})

$$\omega_0 = \frac{1}{2\pi} \sqrt{\frac{K_{\text{eff}}}{M_{\text{eff}}}}$$

The resonator springs are composed of eight coupled springs with identical rectangular cross-sections. We can therefore use the beam deflection equation for a perpendicularly loaded cantilever beam, with its free end allowing no rotation (i.e. the slope of the beam at its free end equals zero), to derive the effective spring constant (K_{eff}). The maximum deflection relation for a single spring is given:

Applied spring force = (F)

The product of spring deflection = (Y_0)

Spring stiffness constant = (K)

The moment of inertia = (I)

Young's Modulus = (E)

Beam length = L

$$\text{Deflection} = Y_0 = \frac{FL^3}{12EI}$$

Since the applied spring force (F) is equivalent to the product of spring deflection (Y_0) and spring stiffness constant (K), and the moment of inertia (I) for a beam of rectangular cross-section can be represented as given:

$$I = \frac{1}{12}tw^3 \quad \text{Simplified and rewritten:} \quad K = \frac{Etw^3}{L^3}$$

The moment of inertia = (I)

Layer thickness = (t)

Spring width = (w)

By separately summing, in series or parallel as required, the spring constants for the other seven springs, an effective spring constant is obtained as given

Spring constant = (K_{eff})

$$\text{Layer thickness} = (t) \quad K_{eff} = \frac{2Etw^3}{L^3}$$

Spring width = (w)

The weight of the springs and trusses can account for as much as 4 - 5% of the resonant frequency value. The kinetic energy equivalence method was employed to derive an effective mass parameter for the comb drive resonator system. Below represents the mass of the system for determining resonant frequency.

Mass constant = (M_{eff})

Mass of shuttle = ($M_{Shuttle}$)

Mass of springs = ($M_{Springs}$)

Mass of truss = (M_{Truss})

$$M_{eff} = M_{Shuttle} + \frac{12}{35}M_{Springs} + \frac{1}{4}M_{Truss}$$

It is important to note that the spring width, w , presents the dimension most sensitive to change. A slight change in the spring width dimension has a relatively large effect on the spring constant and therefore, resonant frequency. Also, note that layer thickness, t , has no effect on the resonant frequency since it may be factored out of K_{eff} and M_{eff}

($M_{eff} = \rho t A_{eff}$) then canceled.

$$\omega_0 = \frac{1}{2\pi} \sqrt{\frac{Ew^3}{\rho L^3 \left(A_{Shuttle} + \frac{12}{35} A_{Springs} + \frac{1}{4} A_{Truss} \right)}}$$

Resonant frequency = (ω_0)

Mass constant = (M_{eff})

Area of shuttle = $(A_{shuttle})$

Area of springs = $(A_{springs})$

Area of truss = (A_{truss})

Density = (ρ)

Young's Modulus = (E)

Spring width = (w)

Reference

Serway, Raymond A. Principles of Physics. Fort Worth: Saunders College, 1994. 674-675.

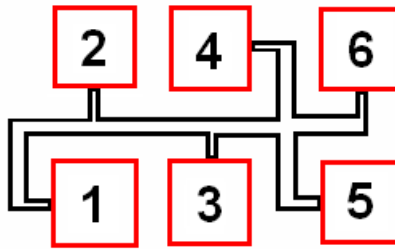
Danelle M. Tanner, Norman F. Smith, Lloyd W. Irwin, William P. Eaton, Karen S. Helgesen, J. Joseph Clement, William M. Miller, Jeremy A. Walraven, Kenneth A. Peterson, Paiboon Tangyonyong, Michael T. Dugger, and Samuel L. Miller, January 2000, "MEMS Reliability: Infrastructure, Test Structures, Experiments, and Failure Modes", Sand Report SAND2000-0091.

Danelle M. Tanner, Albert C. Owen, Jr, and Fredd Rodriguez "Resonant frequency method for monitoring MEMS fabrication", Sandia National Laboratories, SPIE's Proceedings, Volume 4980, Reliability, Testing, and Characterization of MEMS/MOEMS, San Jose, CA, January, 2003, pp 220 -228

Split-Cross Bridge

Comb resonator spring width is somewhat difficult to measure; a separate test structure was used to examine linewidth as a function of position on the wafer. Theoretically, the linewidth relates to the spring stiffness, in that it is cubed with thickness. The split-cross-bridge resistor structure was used to measure line width. This structure also has a van der Pauw built into it through pads 3, 4, 5 and 6. So the same device can be used to measure sheet resistance and line width. The edge bias should be the same for the split-cross bridge and the resonator beams. A general schematic of the split-cross-bridge resistor is given below.

Operation



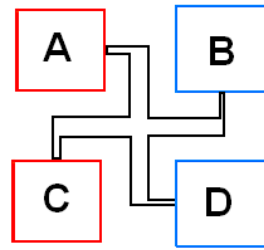
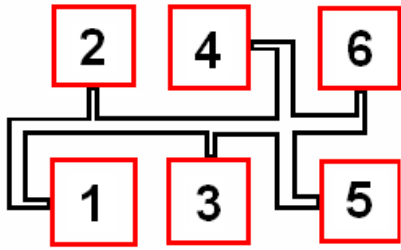
To electrically measure linewidth, apply a current of 1 mA across contact pads 1 and 6 and measure the voltage drop across contact pads 2 and 3. Next, to reduce measurement error, reverse the direction of the current and measure the voltage drop again.

To find the sheet resistance four measurements need to be taken. A current of 1 mA is applied between pads 3 and 5 and the voltage between pads 4 and 6 is taken. Then, the direction of the current is reversed and the voltage is read again. Finally, the current is applied between pads 4 and 6 and the voltage between pads 3 and 5 is taken, again with current in one direction and then the other.

To Measure Linewidth		
Measurement	Applied 1 mA Of Current	Measurement Of Voltage
1	1 & 6	2 & 3
To Measure Sheet Resistance		
Measurement	Applied 1 mA Of Current	Measurement Of Voltage
2	3 & 5	4 & 6
3	5 & 3	4 & 6
4	4 & 6	3 & 5
5	6 & 4	3 & 5

Technical Details

Calculating Sheet Resistance



The split-cross-bridge (above left) has a van der Pauw (above right) built into it through pads 3, 4, 5 and 6. So the same device can be used to measure sheet resistance and line width. To read more about this please refer to the contact resistance section.

Calculating Linewidth

The Greek cross is used to measure the sheet resistance. Current is then passed between 1 and 5 and the voltage is measured between 4 and 6. The resistance $R_{4,6}$ is then calculated. The linewidth is then found using this value.

Measuring the Overlay Error

Masks are aligned to one another using special patterns located on each mask. Alignment errors can result from bad stepping, lithography equipment or wafer distortion. These errors are also known as overlay errors.

A current is passed between the contact pads I_1 and I_2 . The voltage measuring points (shown by the arrow) are spaced equal distances apart. The conductor mask defines V_1 , V_2 and V_4 , while V_3 is defined by the contact mask.

For no misalignment error:

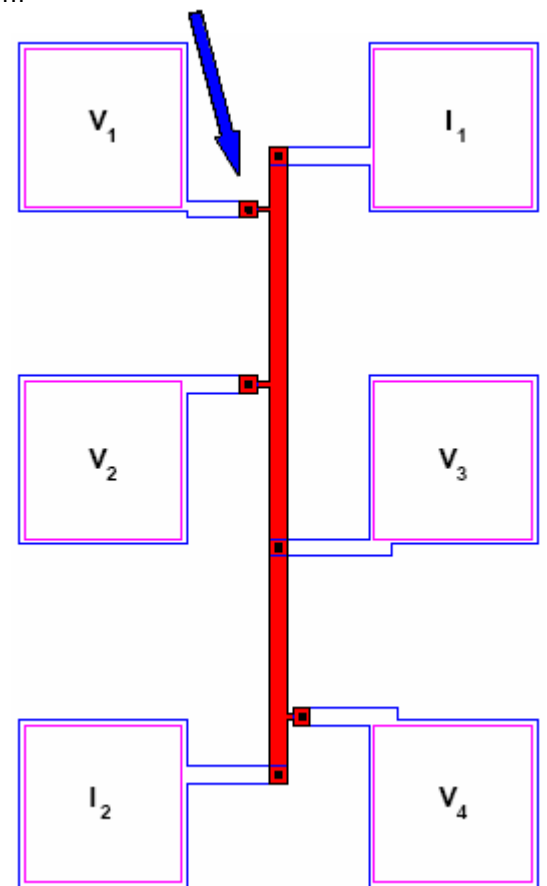
$$(V_4 - V_3) = (V_3 - V_2) = (V_2 - V_1)$$

$$y = \text{Linewidth}^{\text{th}}$$

$$R = \text{Resistar}$$

$$L = \text{Length}$$

$$y = \frac{R_{4,6}}{R_s L}$$



The difference in voltage ΔV is given by:

$$\Delta V = (V_1 - V_2) - (V_2 - V_3) \quad (9)$$

$$\Delta V = (V_1 - V_2) - (V_3 - V_4) \quad (10)$$

The resulting sign of ΔV will depend upon the direction of the overlay error. Let S = spacing between the measurement points. The error in alignment is given by:

$$error = \frac{\Delta V * S}{V_4 - V_3}$$

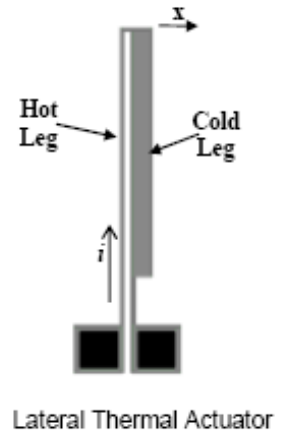
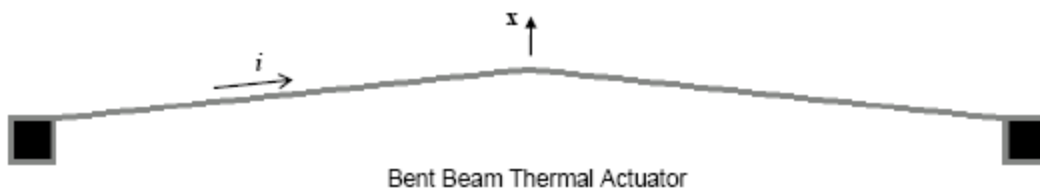
A similar structure turned 90° will give the overlay error in the direction of the short axis.

Reference

“Microelectronic Test Structures” *A.J. Walton*, Edinburgh Microfabrication Facility
Department of Electrical Engineering Kings Buildings, University of Edinburgh
Edinburgh, EH9 3JL, UK <www.see.ed.ac.uk/research/IMNS/papers/micro_test.pdf>.

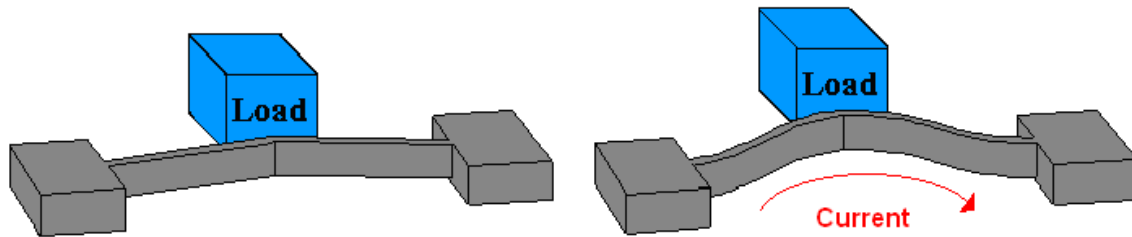
Thermal Actuator with Restoring Spring Force

Thermal expansion is the tendency of matter to change in volume in response to a change in temperature. The degree of expansion divided by the change in temperature is called the material's coefficient of thermal expansion and generally varies with temperature. In a thermal actuator, heat is used to cause the expansion of components to create movement. When a voltage is applied to a thermal actuator it heats up and exerts a "push" or "pull" force. When the voltage is removed the actuator cools down and returns to its original position. The spring represents a load that the actuator can act upon. The center of the beam is offset slightly to control the direction of deflection.



Operation

Bond Pad Information				
Bond Pad Number	Input Signal Label	Input Signal Frequency	Input Voltage Peak to Peak	Waveform
5	Ground		NA	
6	Input	Maximum 250Hz	5Vpp with +2.5V offset or 10Vpp with +5V offset	Square



Technical Details

To completely analyze thermal actuators finite analysis needs to be applied (thermal actuators are not linear). Thermal actuators are nonlinear, although linear approximations can be made for each particular actuator. These approximations can then be used to illustrate the trade-offs of the actuator design with respect to the actuator length, angle and cross-sectional area.

Young's Modulus

Young's modulus (E) is defined as the ratio of the rate of change of stress with strain. This can be experimentally determined from the slope of a stress-strain curve created during tensile tests conducted on a sample of the material. Young's Modulus affects both the displacement and output force predicted by the model. Its magnitude will be a function of the fabrication process.

Resistivity

Resistive heating is used to drive the thermal actuator. Because thermal actuators can reach temperatures above 600° C, this property should be known as a function of temperature. Polysilicon resistivity is measured using standard van der Pauw sheet-resistance structures (refer to Contact Resistance and Split-Cross Bridge sections) from room temperature up to 550° C. At room temperature the resistivity is 21.5 ohm-microns.

Thermal Conductivity

The thermal conductivity of the structural material and the surrounding environment should be known as a function of temperature. At room temperature the thermal conductivity of polysilicon is 72 W/m/°C (this decreases with increasing temperature). At room temperature the thermal conductivity of air is 0.026 W/m/°C (this increases with increased temperature).

Coefficient of Thermal Expansion (CTE)

The instantaneous coefficient of thermal expansion has been measured on single crystal silicon up to 1500° K. To calculate the total elongation due to a temperature change, the instantaneous CTE must be integrated across the temperature range.

$$L - L_0 = L_0 \int_{T_0}^T \alpha_l(T) dT$$

L_0 = the zero - stress length at T_0

L = the new length at T

At room temperature the CTE of polysilicon is $2.5 \times 10^{-6} \text{ } ^\circ\text{C}^{-1}$ and it increases with temperature.

Using Euler Column Formula for Buckling:

The following buckling equations are assuming that the thermal actuator is made up of straight legs. So this is a linear approximation, when in reality the thermal actuator's legs are curved.

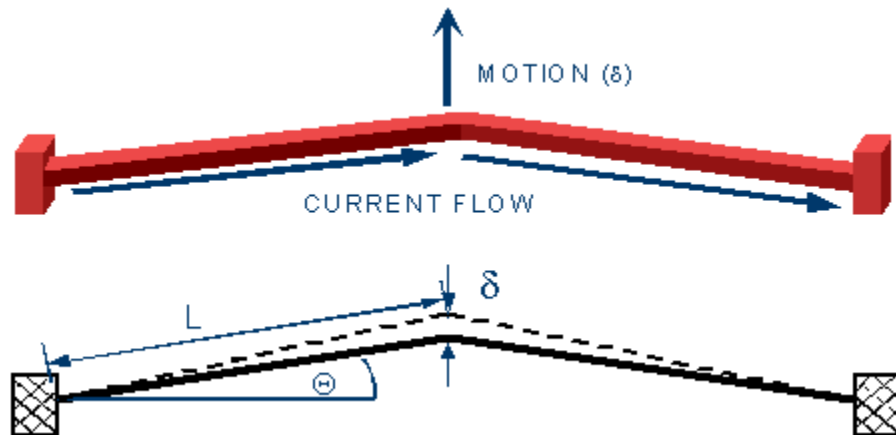
$$F_{cr} = \frac{4\pi^2 nEI \sin \theta}{L^2}$$

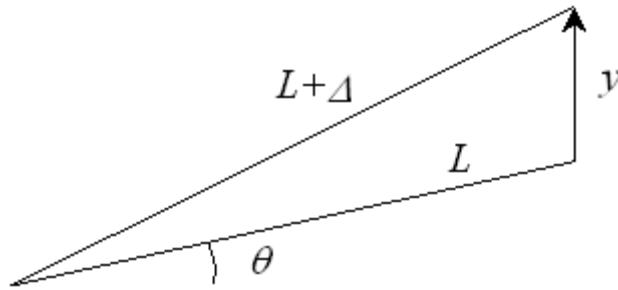
F_{cr} = Critical buckling load or elastic stability limit E = Young's modulus

I = Area moment of inertia of the cross - section

L = Length of the column

F = Force

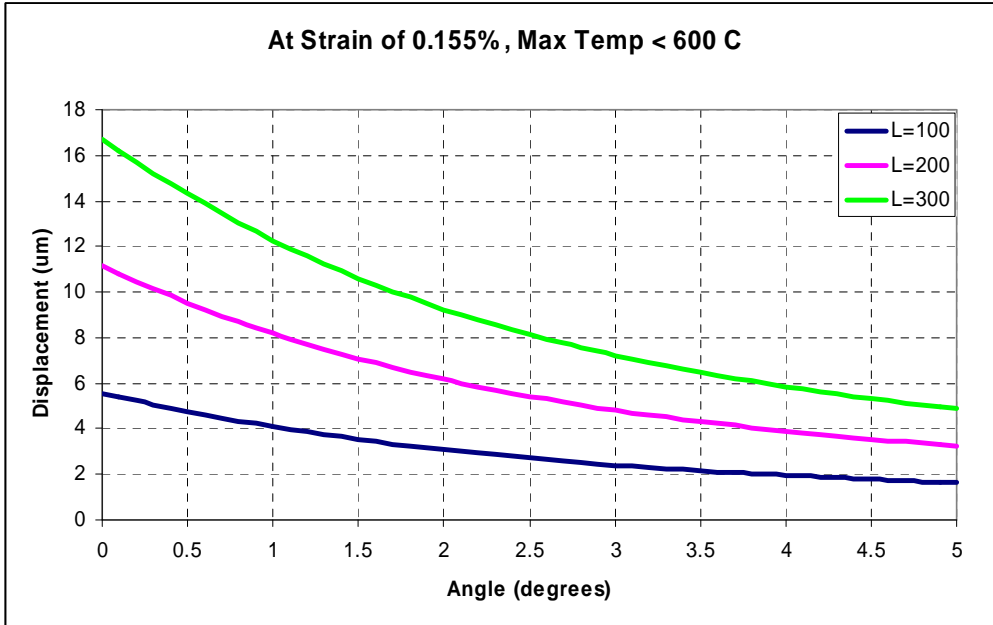




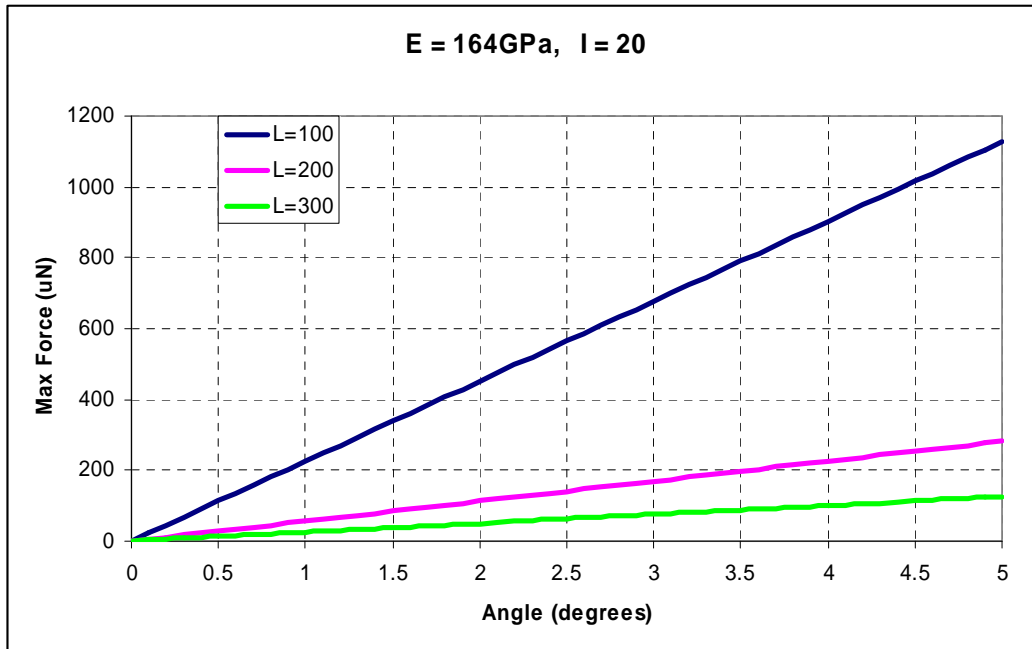
Simplified representation of actuator displacement.

$$y = \sqrt{(L + \Delta)^2 - (L \cos \theta)^2} - L \sin \theta$$

The graph below shows that amplification of $>20X$ can be achieved by constraining the expansion at a small angle. The trade-off is output force. Thermal expansion of each half-leg is $<0.5 \mu\text{m}$.



Output force is determined by the critical buckling force of the actuator leg. Force can be increased at the expense of operating power by increasing number of legs or leg cross-sectional area.



Reference

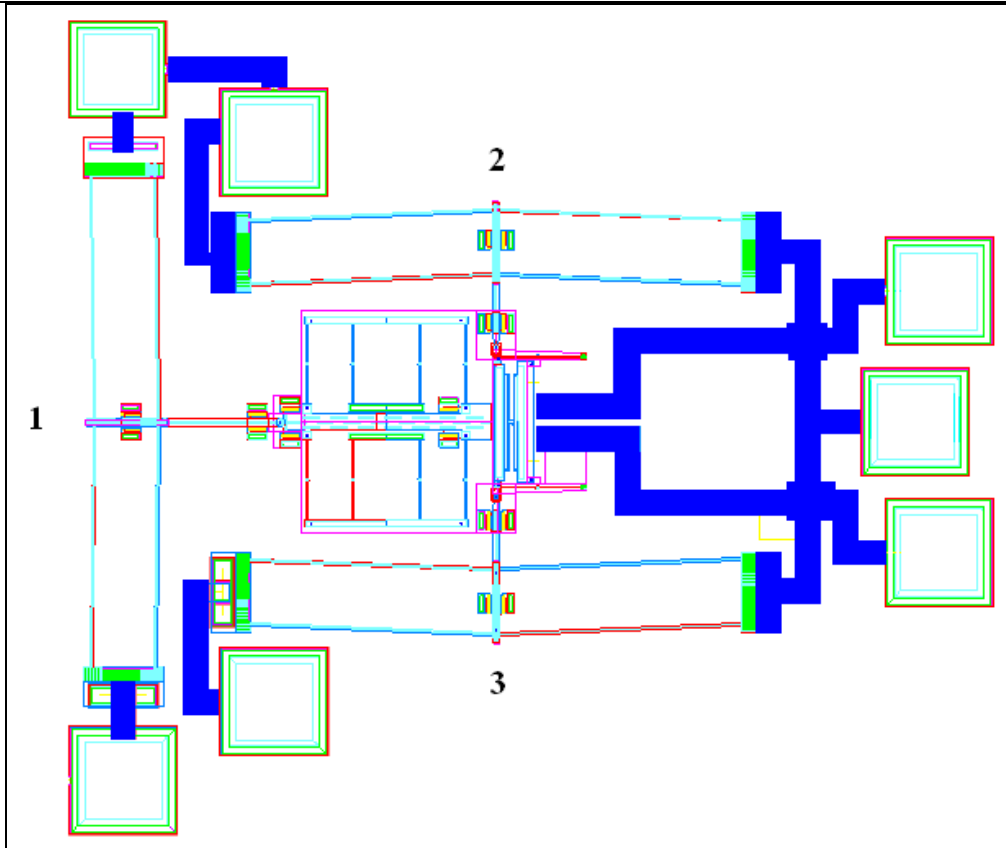
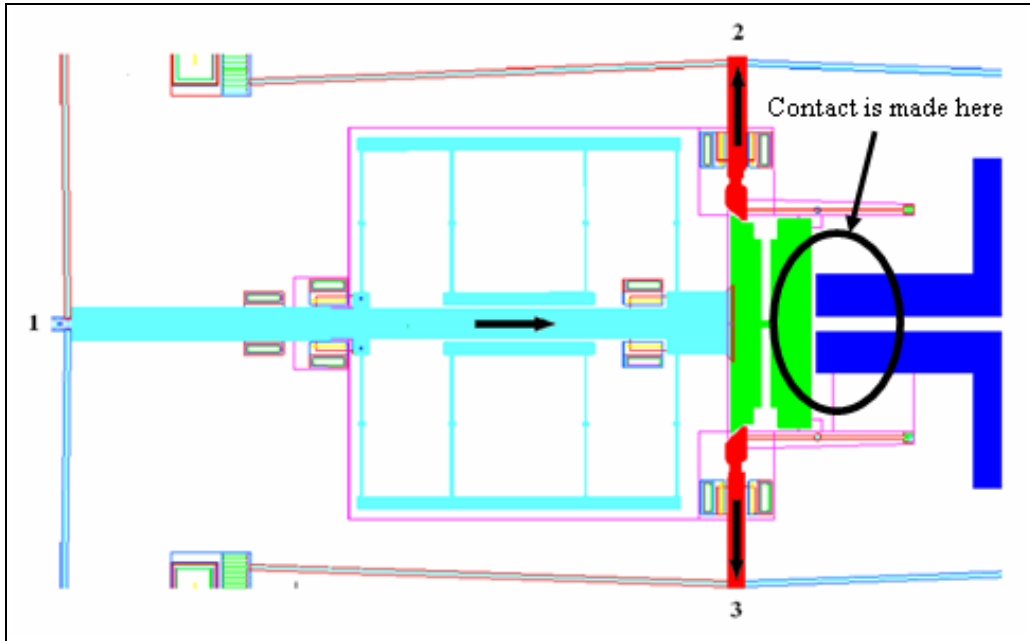
Beer, Ferdinand P., and Russell Johnston Jr. Mechanics of Materials. 2nd ed. New York: McGraw-Hill, Inc., 1992. 24-47.

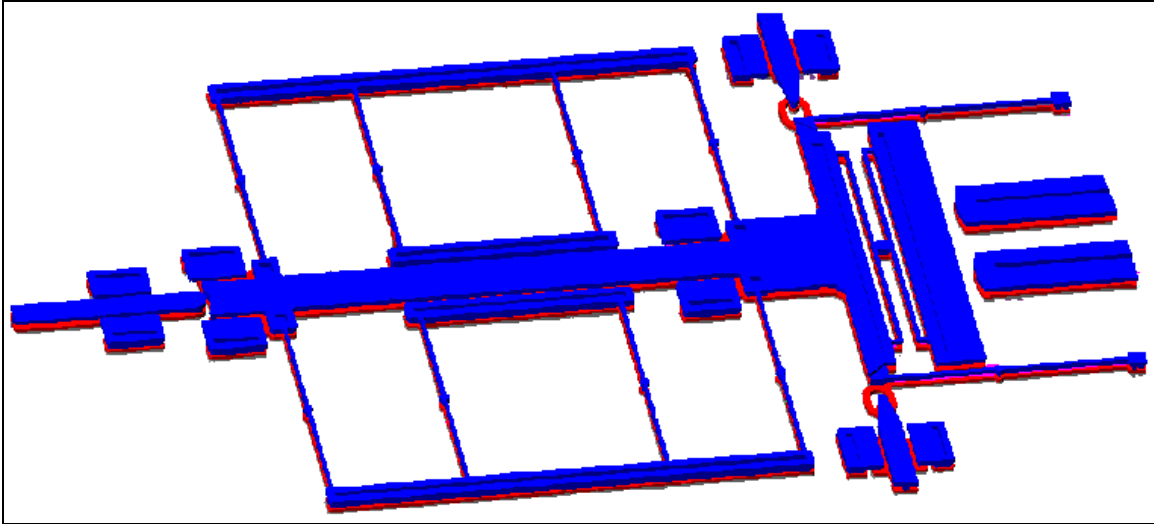
Baker, M.S., Plass, R.A., Headley, T.J., and Walraven, J.A., 2004, "Final Report: Compliant Thermo-Mechanical MEMS Actuators LDRD #52553," Sand Report SAND2004-6635.

Thermally Actuated Latching Switch

In basic electronics there are two types of circuits: open and closed. The terms "open" and "closed" refer to the circuit's current path and whether it is interrupted or not. When the circuit is complex and made up of various parts, being able to interrupt the current path independently from other parts can greatly reduce the number of circuit inputs needed. The next logical step in this process would be to allow the interrupt of the current path to be reversed; this concept brings us to the switch. A latching switch can be activated once or "set into position", and then activated again to return to its original position. This is similar to flipping on a light switch and the light staying on, instead of having to hold the switch to the on position for the entire time you want the light on.

The latching switch in this module is actuated by a thermal actuator. To unlatch the switch 2 more actuators are used. When activated, actuator 1 applies a force to the switch, moving it toward the traces (shown in the figure as dark blue). On either side of a switch there are clips. When the switch bar slides past these two clips it is held in place making contact with the traces. At this point the switch is latched into place, creating a closed circuit. At this point there is no need for actuator 1 to apply any force, so it can be deactivated. To unlatch the switch and re-open the circuit actuators 2 and 3 will be actuated. These two actuators apply opposite perpendicular forces to the clips moving them away from the switch. This allows the switch to move away from the traces, which opens the circuit. After the switch has moved away from the traces actuators 2 and 3 no longer need to be actuated.





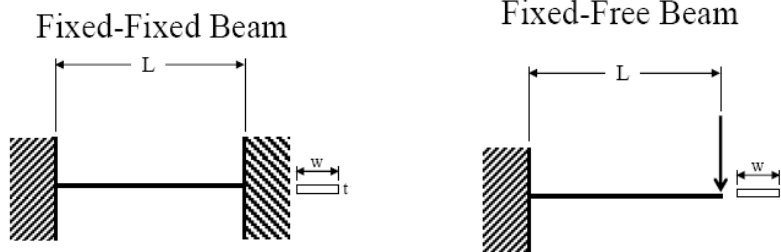
This thermal switch contains 3 thermal actuators. One of the actuators (labeled 1 in figures) exerts a horizontal force. This horizontal force pushes the switch past the latches into the closed position causes the switch to make contact with the traces. The second and third actuators are perpendicular to the first actuator. These two actuators work in conjunction by exerting forces, opposite to each other, in the vertical direction.

When voltage is applied, these two actuators pull the two latching clips away from the center, allowing the switch to spring back into the open position. The horizontal actuator is not connected to the switch, so even with the switch latched in the closed position; the actuator is free to return to its natural position when voltage is not applied. The latches are not rigidly connected to the two side actuators, so they are free to move out of the way as the switch pushes past. The side actuators are able to pull on the latches, but that is all, they don't interfere with the free motion of the latches.

Operation

Ground pins 9 and 11 then apply voltage to pin 10 to power the “latch” actuator. Gradually ramp up the voltage, starting at 5V until you see the contact latch close. Watch the two latches. You will see the contact push past them and they'll spring back to their fabricated position. Once this happens, turn off the actuator and make a note of the voltage. Next, apply a voltage to pin 8 to pull the latches apart. Again, start at 5V and ramp up the voltage, slowly, until the contact springs open. Thermal actuators draw significant current, in the 10's of milliamps. Therefore, make sure to use a power supply capable of sourcing enough current and that at the compliance current is not set too low.

Technical Details



$$\text{Stress} = \frac{\text{Applied Load}}{\text{Cross - Sectional Area}} = \sigma$$

$$\text{Strain} = \frac{\text{Change in Length of Material}}{\text{Original Length of Material}} = \epsilon$$

You will have to account for buckling When $F > F_{cr}$

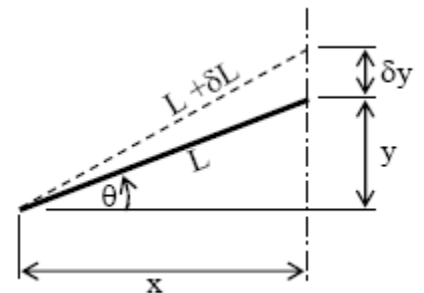
Bent Beam Thermal Actuator Displacement Amplification:

Using $x^2 + y^2 = L^2$

Where: $y = y + \delta y$ and $L = L + \delta L$

$$x^2 + (y + \delta y)^2 = (L + \delta L)^2$$

Mechanical Amplification: $\frac{\delta y}{\delta L} \cong \frac{L}{y} \cong \frac{1}{\theta}$



θ	$\delta y / \delta L$
1°	57.3
2.5°	22.9
5°	11.5
10°	5.8

Torsional Ratchet Actuator with braking system (TRA)

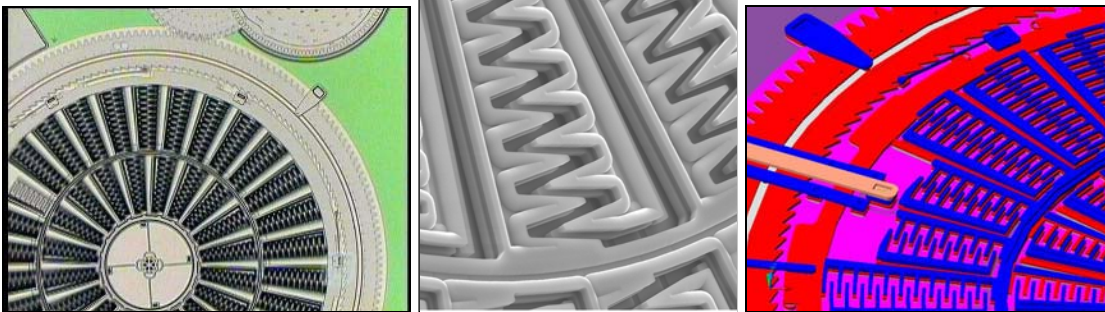
The TRA uses rotational comb drives for electrostatic operation a large circular frame ties the movable banks of combs together. Four cantilever beams support this frame in its center and act as the frame's spring return. These four beams are resistant to any lateral motion of the frame but allow it to rotate. The frame is limited to 2.8° of rotation by stiff spring stops at its outside edge. To avoid stiction problems, the frame has dimples fabricated in its bottom surface.

The torsion frame is surrounded by a ring gear, four overhanging clips, ratchet pawls, and three anti-reverse mechanisms. The ring gear has standard gear teeth on its circumference. The overhanging clips hold the frame to the substrate. The inside of the ring gear is lined with a rack of ratchet teeth. Equally spaced around the edge of the torsion frame are three ratchet pawls that engage with the ratchet teeth. To prevent any unwanted reverse motion of the gear, there are three anti-reverse mechanisms, which are anchored cantilever beams. The frame is connected to the ground plane at the central torsion springs.

The stationary sections of the comb banks are connected using electrically isolated pieces of the ground plane. A connection to the stationary banks of combs is made using a signal line that passes above the gear and connects with one of the stationary comb banks. To actuate the TRA, a periodic voltage signal is applied to the stationary combs. As the signal voltage increases, the torsion frame rotates counterclockwise about its springs. This is in response to the electrostatic attraction between the stationary and moving comb fingers. When the voltage is removed, the central torsion springs force the frame to return to its fabricated position.

This type of actuator has many inherent advantages.

- 1) High density of electrostatic force elements
 - a) The result of a compact overall actuator layout
 - b) This density minimizes the voltage required and area consumed
- 2) The ring gear is only ratcheted in one direction; the TRA requires only two electrical connections to run
- 3) Operates on extremely simple input signals
- 4) Ratcheting system produces discrete displacement outputs.
 - a) The actuator can be used for open loop positioning of a load.



Operation

Bond Pad Information					
Bond Pad Number	Input Signal Label	Input Signal Frequency	Input Voltage Peak to Peak	Waveform	Other
Torsional Ratchet Actuator					
21	Ground	0	0	Not Used	
22	Input	< 1 Hz - 1 kHz	15 - 55 V	Clipped Square	
Torsional Ratchet Actuator Brake					
21	Ground	0		Not Used	
20	Input	DC or Square	0 - 55 V	Clipped Square or DC	Variable to adjust break pressure

Displacement Range: up to 40μm

Force Range: 500 μN

Technical Details

Motion

A voltage difference produces an attractive force between the combs. By applying voltages to the four inputs (two per actuator), a circular motion is produced. The X and Y linkage arms are connected to the gear via a pin joint. The gear rotates around a hub. The Microengine uses electrostatic attraction, which causes two objects at different potentials to induce motion. These electrostatic forces attract but do not repel the shuttle. Due to this attraction both sides of the shuttle need to be acted upon for the shuttle to move in both directions.

System Model

Model-based design parameters that will result in low voltage operation require appropriate system models. The model for the system is based on:

$$T_{IC} = (V, \theta) + T_{OC}(V, \theta) - T_S(\theta) = I \frac{d^2\theta}{dt^2}$$

T_{IC} = torque produced by the inner banks of comb fingers

T_{OC} = torque produced by the outer banks of comb fingers

T_S = resisting torque of the center torsion springs,

I = moment of inertia of the torsion frame

θ = angular displacement of the torsion frame

V = applied voltage
t = time

To account for the linear clamping of the comb banks that occurs at the end of each comb's travel, equation (2) must be used.

Summing the individual torque contributions of each comb finger yields:

$$T_{IC}(V, \theta) = \beta n \sum_{combs} \left[\left(\frac{A}{2g_t(\theta)^2} + \frac{h}{g_s} \right) \epsilon r V^2 \right]$$

n = number of inner comb banks
A = area of the tip of the comb
g_t = parallel plate gap between the end of a finger and the root of the opposing comb
h = vertical thickness of the combs
g_s = gap between adjacent comb fingers
ε = dielectric constant for air
r = radius of the individual comb finger

The β term in equation 2 accounts for the decrease in the capacitance of the electrostatic combs due to the underlying ground plane

Tang shows this term can be approximately 0.7, which represents a 30% reduction in the force output of the combs.

All calculations in this analysis use 0.7 for β. There is a similar expression for T_{oc}.

Due to the complicated spring displacement and geometry, a three-dimensional non-linear finite element analysis (FEA) was performed to calculate their stiffness. The finite element model used was of a single cantilever and its strain relief structures. The boundary conditions used were deflection and angle specifications at the free end of the spring and fixed conditions at the base of the spring. The total end moment required to deflect the beam to the end conditions was calculated at one degree displacements. A polynomial fit was then used to find the torque-deflection relationship:

$$=149q + 11.8q^2 - 1.65q^3 \text{ s } T (3)$$

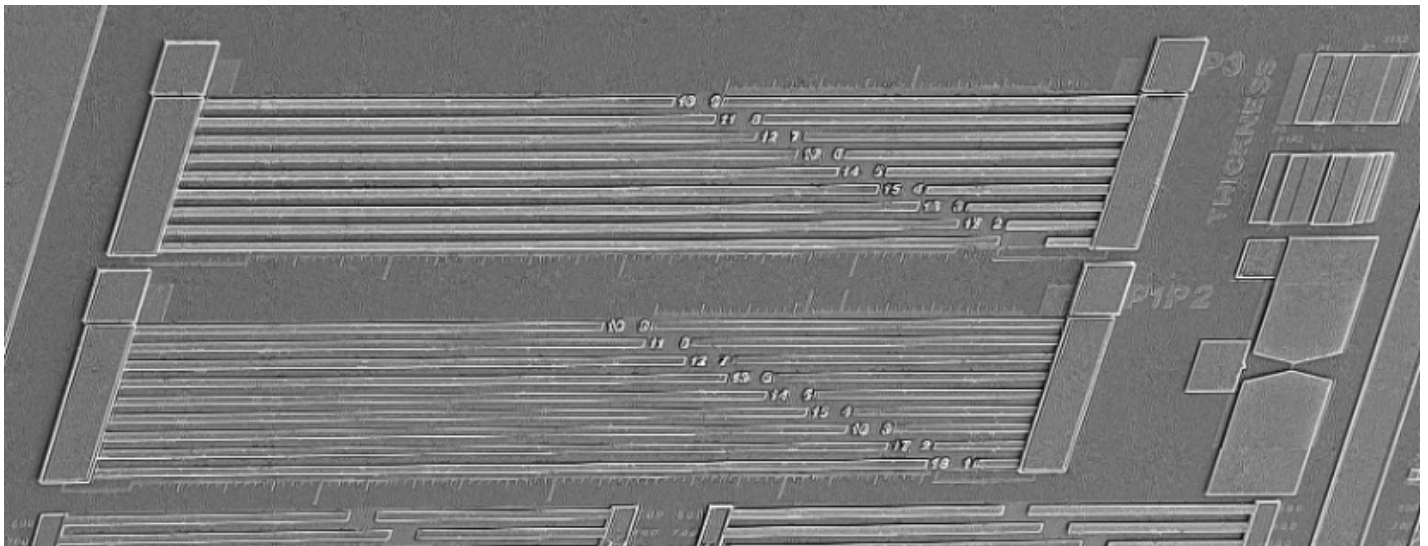
Reference

Stephen M. Barnes, Samuel L. Miller, M. Steven Rodgers, Fernando Bitsie, "Torsional Ratcheting Actuating System" SAND Report SAND2000-0203C.

Variable Length Cantilevers

Variable length cantilevers are used to measure adhesion, z-axis stress gradient, and Young's modulus. The cantilever beams are used for a wide variety of diagnostic procedures. Two large groups include beams from 100 microns to 1800 microns long, in increments of 100 microns are present on these die. The beams are a laminate of MMPoly1 and MMPoly2 layers

Cantilever beam example



Operation

Beams	Bond Pad Number	Input Signal Frequency	Input Voltage Peak to Peak	Waveform
Smaller set of Beams (1-9)	18	Ground	NA	NA
	19	Power	Variable (20V begins to pull Down smaller beams)	DC voltage
Longer set of Beams (10-18)	18	Ground	NA	NA
	16	Power	Variable (~80V)	DC voltage

Young's modulus can be measured by taking an interferometric measurement of beam deflections for electrostatically loaded beams. The beam's deflected shape may then be modeled, and the value of Young's modulus that minimizes the difference between the measured and modeled deflections may be extracted.

Technical Details

Crack Length Used to Measure Adhesion Energy

Cantilever beams can be used to find surface adhesion. This can be measured by applying a voltage to the actuating pad and causing the beams to touch the underlying ground layer. When the voltage is released, surface adhesion will prevent the longer beams from separating from this ground plane. Measurements of the adhered length of the beam allow determination of the surface adhesion.

To Measure Z-axis Stress Gradient

Z-axis stress gradient is measured on any of the five banks of beams using an interferometric measurement of deflection of unloaded beams. Internal moments due to the stress gradient cause the beam to curl into a circular arc. The radius of which indicated the amount and direction of z-axis stress-gradient.

The radius of curvature can be approximated by the following equation:

$$R \cong \frac{L^2}{2\delta} = \frac{L^2}{\lambda N_f}$$

Equations for the stress gradient:

$$\gamma = \frac{E}{R}$$

Where:

Beam length = L

Out-of-plane deflection of the end of the beam equal to the wavelength $\lambda \approx 546 \text{ nm} = \delta$

Number of fringes = N_f

Young's Modulus = E

Reference

Baker, M.S., Plass, R.A., Headley, T.J., and Walraven, J.A., 2004, "Final Report: Compliant Thermo-Mechanical MEMS Actuators LDRD #52553," Sand Report SAND2004-6635.

UA Module Bond Pad Legend

Bond Pad	Device	Voltage Applied
1	Linear Comb Drive Micro Engine	Voltage
2	Linear Comb Drive Micro Engine	Voltage
3	MMPoly4 Resonator	Voltage
4	MMPoly4 Resonator	Ground
5	Thermal Actuator with Restoring Spring Force	Ground
6	Thermal Actuator with Restoring Spring Force	Voltage
7	MMPOLY3 Resonator	Ground
8	Thermally Actuated Bimodal Latch	Voltage
9	Thermally Actuated Bimodal Latch	Ground
10	Thermally Actuated Bimodal Latch	Voltage
11	Thermally Actuated Bimodal Latch	Ground
12	MMPoly 1 & 2 Resonators	Ground
13	MMPoly 1 & 2 Resonators	Voltage
14	Not Used	Not Used
15	MMPOLY3 Resonator	Voltage
16	Variable Length Cantilevers	Voltage
17	Not Used	Not Used
18	Ground/ Nitride Cut	Not Used
19	Variable Length Cantilevers	Ground
20	Torsional Ratcheting Actuator with Brake	Voltage
21	Torsional Ratcheting Actuator with Brake	Ground
22	Torsional Ratcheting Actuator with Brake	Voltage
23	Linear Comb Drive Micro Engine	Voltage
24	Linear Comb Drive Micro Engine	Voltage
25	Linear Comb Drive Micro Engine	Ground
26	Not Used	Not Used

References:

Contact Resistance

Schroder, Dieter K. Semiconductor Material and Device Characterization. New York: John Wiley & Sons, Inc., 1990. 1-14.

“Microelectronic Test Structures” *A.J. Walton*, Edinburgh Microfabrication Facility Department of Electrical Engineering Kings Buildings, University of Edinburgh Edinburgh, EH9 3JL, UK <www.see.ed.ac.uk/research/IMNS/papers/micro_test.pdf>.

Etch Undercut and Nitride Etch Undercut Structures

“Release-etch modeling for complex surface micromachined structures”, W.P. Eaton, J.H. Smith, R.L. Jarecki, Sandia National Laboratories, Micromachined Devices and Components, Proceedings of the SPIE, Vol 2882, Austin, TX, Oct 14-15, 1996.

Linear Comb Drive Micro Engine

Image from: Moussa, W.A., H Ahmed, W Badawy, et al. "Investigating the Reliability of Electrostatic Comb-Drive Actuators Used in Microfluidic and Space Systems Using Finite Element Analysis." Canadian Journal of Electrical and Computer Engineering 27 (2002): 195-200.

Ted Dellin “Electrostatics and Comb Drives” Power Point, 2005

MEMS “Pull Tab” Tensile Strength Structures

Beer, Ferdinand P., and Russell Johnston Jr. Mechanics of Materials. 2nd ed. New York: McGraw-Hill, Inc., 1992. 24-47.

Resonator

Serway, Raymond A. Principles of Physics. Fort Worth: Saunders College, 1994. 674-675.

Danelle M. Tanner, Norman F. Smith, Lloyd W. Irwin, William P. Eaton, Karen S. Helgesen, J. Joseph Clement, William M. Miller, Jeremy A. Walraven, Kenneth A. Peterson, Paiboon Tangyonyong, Michael T. Dugger, and Samuel L. Miller, January 2000, “MEMS Reliability: Infrastructure, Test Structures, Experiments, and Failure Modes”, Sand Report SAND2000-0091.

Danelle M. Tanner, Albert C. Owen, Jr, and Fredd Rodriguez “Resonant frequency method for monitoring MEMS fabrication”, Sandia National Laboratories, SPIE’s Proceedings, Volume 4980, Reliability, Testing, and Characterization of MEMS/MOEMS, San Jose, CA, January, 2003, pp 220 -228

Split-Cross Bridge

“Microelectronic Test Structures” *A.J. Walton*, Edinburgh Microfabrication Facility
Department of Electrical Engineering Kings Buildings, University of Edinburgh
Edinburgh, EH9 3JL, UK <www.see.ed.ac.uk/research/IMNS/papers/micro_test.pdf>.

Thermal Actuator with Restoring Spring Force

Beer, Ferdinand P., and Russell Johnston Jr. *Mechanics of Materials*. 2nd ed. New York:
McGraw-Hill, Inc., 1992. 24-47.

Baker, M.S., Plass, R.A., Headley, T.J., and Walraven, J.A., 2004, “Final Report:
Compliant Thermo-Mechanical MEMS Actuators LDRD #52553,” Sand Report
SAND2004-6635.

Torsional Ratchet Actuator with Breaking System (TRA)

Stephen M. Barnes, Samuel L. Miller, M. Steven Rodgers, Fernando Bitsie, “Torsional
Ratcheting Actuating System” SAND Report SAND2000-0203C.

Variable Length Cantilevers

Baker, M.S., Plass, R.A., Headley, T.J., and Walraven, J.A., 2004, “Final Report:
Compliant Thermo-Mechanical MEMS Actuators LDRD #52553,” Sand Report
SAND2004-6635.